Charge-Transfer Photochemistry of Aromatic π-Complexes. Hexamethylbenzene and Mercuric Trifluoroacetate

W. Lau and J. K. Kochi*

Department of Chemistry, University of Houston, University Park, Houston, Texas 77004

Received October 30, 1985

The π-complex of hexamethylbenzene (HMB) and mercuric trifluoroacetate (HgT_2) is converted with high quantum yields to pentamethylbenzyl trifluoroacetate and either mercurous trifluoroacetate or metallic mercury upon irradiation of the charge-transfer absorption band. X-ray crystallography establishes the charge-transfer (CT) excitation to derive from the η^2-bonding of the mercuric atom to only two of the aromatic carbons of HMB. The CT photochemistry proceeds via the radical-ion pair [$HMB^{+}\cdot$,$HgT_2^{-}\cdot$] in accord with Mulliken theory. The high quantum efficiency is ascribed to the rapid ligand dissociation of $HgT_2^{-}\cdot$ which minimizes the energy wastage due to back electron transfer. The thermal reactions following photoactivation are monitored by following the changes in the CT absorption band and the ESR spectrum of $HMB^{+}\cdot$. The charge-transfer photochemistry of the [HMB,HgT_2] complex shows an unusually high dependency on the solvent—the nature of the mercury-containing products and the quantum yield Φ_P for pentamethylbenzyl trifluoroacetate in dichloromethane being distinctively different from that obtained in trifluoroacetic acid. The formation of metallic mercury with quantum yields in trifluoroacetic acid which can be as high as 3 arises from a radical-chain process which sustains itself after the light is turned off. The critical role played by the mercurous trifluoroacetate radical $\cdot HgO_2CCF_3$ in the CT photochemistry is described.

Aromatic compounds form π-complexes with a variety of electron-deficient organic compounds such as quinones and polynitro- and polycyanoalkenes.[1-3] The formation of these electron donor–acceptor or EDA complexes is often accompanied by colors which vary according to the ionization potential (I_D) of the aromatic moiety.[4] Various π-complexes of arenes with inorganic metal salts are also known.[5] Among these, we were especially attracted to those derived from mercury(II),[6] since they have also been employed as reagents in organic chemistry—mercury(II) trifluoroacetate being a particularly active electrophile in aromatic mercuration.[7]

The organic photochemistry of aromatic π-complexes has especially been of interest to us.[8] In particular, we earlier drew attention to the photoexcitation of EDA complexes in the context of the Mulliken theory of charge transfer.[9,10] Thus the recent successful isolation and structure determination of the EDA complex of hexamethylbenzene and mercury(II) trifluoroacetate[11] presents the opportunity now to examine the chemical consequences of charge-transfer (CT) photoexcitation. As an electron acceptor, mercuric trifluoroacetate poses an interesting problem arising from the transient character of the reduced monomeric mercurous species.

Results

When a solution of an aromatic compound such as toluene is mixed with equimolar amounts of mercuric trifluoroacetate (HgT_2), a flash of yellow color can be observed. The color is more persistent at lower temperatures, and we were able to record the transient absorption from mesitylene at −40 °C in dichloromethane, as shown in Figure 1. In accord with theoretical expectation,[1] the absorption band gradually shifts to progressively lower energies with the decrease in the ionization potential of the aromatic donor—the trend for the series of polymethylbenzenes being as follows: hexamethylbenzene (λ_{max} 315 nm, I_D 7.85 eV); pentamethylbenzene (300 nm, 7.92 eV); 1,2,4,5-tetramethylbenzene (295 nm, 8.05 eV); 1,3,5-trimethylbenzene (288 nm, 8.40 eV). The intensity of the CT absorbances of various arene–HgT_2 complexes in dichloromethane increases with the addition of trifluoroacetic acid, accompanied by a slight blue-shift of the bands. For example, λ_{max} = 305 nm for the [HMB,HgT_2] complex in pure trifluoroacetic acid.

The hexamethylbenzene (HMB) complex with mercuric trifluoroacetate is unique for three reasons. First, the charge-transfer band is shown in Figure 1 to be well separated from the absorption bands of either the uncomplexed HMB donor or the HgT_2 acceptor. Thus we could specifically excite only the CT component of the ground state of the complex [HMB,HgT_2] by direct irradiation through narrow band-pass interference filters. Second, we could successfully prepare the 1:1 EDA complex of HMB and HgT_2. The isolation of the crystalline EDA complex enabled us to relate the molecular structure directly to the charge-transfer excitation. Third, the EDA complex is sufficiently persistent that we could examine the CT photochemistry without any complications from the competing thermal processes.

Molecular Structure of the [HMB,HgT_2] Complex. The slow, controlled removal of the solvent from an equimolar mixture of hexamethylbenzene and mercuric trifluoroacetate dissolved in trifluoroacetic acid afforded a quantitative yield of pale yellow single crystals of the 1:1 EDA complex. The molecular structure shown in Figure 2 represents the first example of an arene–Hg(II) EDA complex that has been definitely characterized by X-ray crystallography.[12] The η^2-bonding of mercury to the

(1) See: Foster, R. *Organic Charge Transfer Complexes*; Academic: New York, 1969.

(2) For reviews, see: (a) Kosower, E. M. *Prog. Phys. Org. Chem.* **1965**, *3*, 81. (b) Colter, A. K.; Dack, M. R. J. *Molecular Complexes*; Foster, R., Ed.; Crane, Russak, & Co.: New York, 1973; Vol. 1, pp 301–362; 1974; Vol. 2, pp 1–61. (c) Andrews, L. J.; Keefer, R. M. *Molecular Complexes in Organic Chemistry*; Holden-Day: San Francisco, 1964.

(3) (a) Mataga, N.; Kubota, T. *Molecular Interactions and Electronic Spectra*; Dekker: New York, 1970. (b) Mataga, N.; Ottolenghi, M. *Mol. Assoc.* **1979**, *2*, 1–78. (c) Masuhara, H.; Mataga, N. *Acc. Chem. Res.* **1981**, *14*, 312.

(4) Fukuzumi, S.; Kochi, J. K. *J. Org. Chem.* **1981**, *46*, 4116.

(5) Tamres, M.; Strong, R. L. *Mol. Assoc.* **1979**, *2*, 368.

(6) (a) Sokolov, V. I.; Bashilov, V. V.; Reutov, O. A. *Dokl. Akad. Nauk SSSR* **1971**, *197*, 101. (b) Fukuzumi, S.; Kochi, J. K. *J. Phys. Chem.* **1981**, *85*, 648. (c) Fukuzumi, S.; Kochi, J. K. *J. Am. Chem. Soc.* **1981**, *103*, 2783.

(7) Larock, R. C. *Organomercury Compounds in Organic Synthesis*; Springer Verlag: Berlin, 1985.

(8) (a) Hilinski, E. F.; Masnovi, J. M.; Kochi, J. K.; Rentzepis, P. M. *J. Am. Chem. Soc.* **1984**, *106*, 8071. (b) Masnovi, J. M.; Huffman, J. C.; Kochi, J. K.; Hilinski, E. F.; Rentzepis, P. M. *Chem. Phys. Lett.* **1984**, *106*, 20. (c) Masnovi, J. M.; Kochi, J. K. *J. Org. Chem.* **1985**, *50*, 5245.

(9) Mulliken, R. S. *J. Am. Chem. Soc.* **1952**, *74*, 811; *J. Phys. Chem.* **1952**, *56*, 801.

(10) Mulliken, R. S.; Person, W. B. *Molecular Complexes*; Wiley: New York, 1969. See also: Nagakura, S. *Excited States*; Lim, E. C., Ed.; Academic: New York, 1975; Vol. 2, p 334.

(11) For a preliminary report, see: Lau, W.; Kochi, J. K. *J. Am. Chem. Soc.* **1982**, *104*, 5515.

0022-3263/86/1951-1801$01.50/0

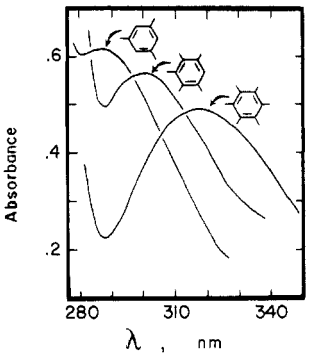

Figure 1. Charge-transfer spectra of 1:1 EDA complexes. Hexamethylbenzene (0.0025 M), pentamethylbenzene (0.0025 M), and mesitylene (0.005 M), each mixed with equimolar amounts of $Hg(O_2CCF_3)_2$ in dichloromethane at −40 °C.

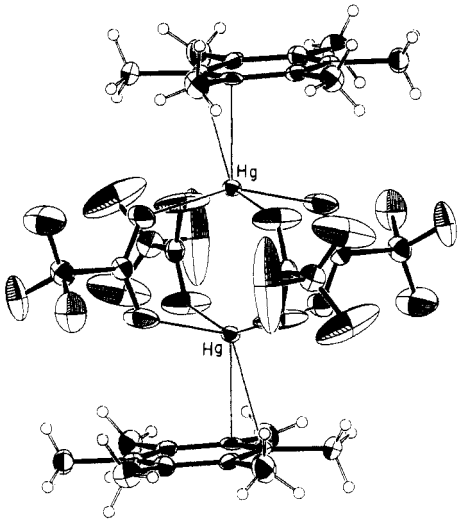

Figure 2. Ortep drawing of the 1:1 EDA complex of hexamethylbenzene and mercuric trifluoroacetate as the dimeric species. Anisotropic thermal ellipsoids are drawn at the 50% probability level. Hydrogen atoms located by difference synthesis and portrayed at 0.5 Å^2.

aromatic ring consists of two unusually long Hg–C distances of 2.56 and 2.58 Å, expected for weak π-interactions in such complexes.[13] The hexamethylbenzene–mercury(II) moiety exists in a dimeric form which is held together with four bidentate trifluoroacetate ligands. The same 1:1 EDA complex was also obtained as a crystalline solid from dichloromethane.

Importantly, the comparison of the absorption spectrum of the crystalline complex with that measured in trifluoroacetic acid indicates the integrity of the CT transition, both in the solid state and in solution.[14] The absorption spectrum of the [HMB,HgT_2] complex in solution (vide infra) is akin to the spectrum of the crystalline complex suspended in a mineral oil mull taken in a transmission mode. The latter showed the CT absorption

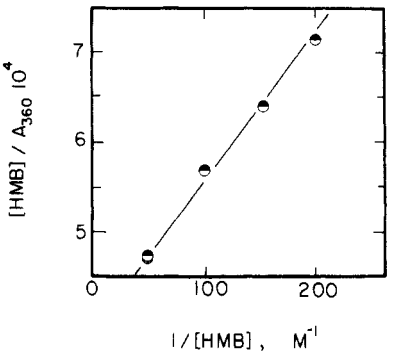

Figure 3. Benesi–Hildebrand plot of hexamethylbenzene and mercuric trifluoroacetate in trifluoroacetic acid at λ = 360 nm with K = 243 M^{-1} and ϵ = 2538 with correlation coefficient 0.997.

with λ_{max} 315 nm but with a slightly broader envelope. Furthermore, the ^1H and ^{13}C NMR spectra of the crystalline complex measured by magic angle spinning accords with those obtained in solution.[15] Typically, the ^{13}C chemical shifts for a solution consisting of a 1:1 mixture of HMB and HgT_2 are 133.0 and 16.6 ppm for the aromatic and methyl carbons, respectively, in dichloromethane and 140.1 and 18.0 ppm in trifluoroacetic acid. The corresponding values for the crystalline 1:1 EDA complex are 135.8 and 17.5 ppm. For free HMB, the values are 131.7 and 16.5 ppm (or 134.7 and 16.8 ppm) in dichloromethane (or trifluoroacetic acid) and 132.3 and 17.4 ppm in the crystalline solid.[16,17] For the NMR spectra of the [HMB,HgT_2] in solution,[18] see the Experimental Section.

Formation Constant of the [HMB,HgT_2] Complex in Dichloromethane and Trifluoroacetic Acid Solutions. The charge-transfer absorption band of the [HMB,HgT_2] complex at $\lambda_{max} \sim 310$ nm was observed immediately upon mixing solutions of hexamethylbenzene and mercuric trifluoroacetate in either dichloromethane or trifluoroacetic acid. The formation constants of the EDA complex in these solvents was measured spectrophotometrically by the Benesi–Hildebrand procedure.[19] For the formation of the 1:1 complex, i.e., eq 1, the changes

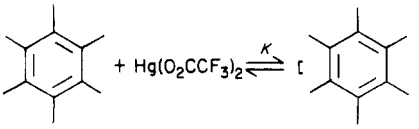

(1)

in the absorbance A_{CT} of the CT band at various concentrations of the donor and acceptor are given by[1] eq 2 under conditions in which [HMB] ≫ [HgT_2]. The data pres-

$$\frac{[HgT_2]}{A_{CT}} = \frac{1}{\epsilon_{CT}} + \frac{1}{K\epsilon_{CT}[HMB]} \qquad (2)$$

ented in Figure 3 yield ϵ and K from the intercept and slope, respectively. The values of the extinction coefficient of ϵ 2320 and 2510 M^{-1} cm^{-1} identify the complex to be essentially the same in dichloromethane and trifluoroacetic acid. The formation constants of K = 16 and 243 M^{-1}

(12) For the structures of the the somewhat related arene–silver(I) complexes, see: Rundle, R. E.; Goring, J. H. *J. Am. Chem. Soc.* **1950**, *72*, 5337. Smith, H. G.; Rundle, R. E. *Ibid.* **1958**, *80*, 5075. Griffith, E. A. H.; Amma, E. L. *Ibid.* **1971**, *93*, 3167 and related papers. (d) For a summary of arene complexes, see ref 4 and: Herbstein, F. H. *Perspectives in Structural Chemistry*; Dunitz, J. D., Ibers, J. A., Eds.; Wiley: New York, 1971; Vol. 4, pp 166ff.

(13) The length of σ-bonds between mercury and carbon are typically 2.1–2.2 Å. Compare: Kamenar, B.; Penavic, M. *Inorg. Chim. Acta* **1972**, 6, 191. For some examples of π-bond lengths, see: Canty, A. J.; Chaichit, N.; Gatehouse, B. M. *Acta Crystallogr., Sect. B* **1980**, *B36*, 786. Lampe, P. A.; Moore, P. *Inorg. Chim. Acta* **1979**, *36*, 27.

(14) For other examples of charge transfer in the solid state, see: Soos, Z. G.; Klein, D. J. *Mol. Assoc.* **1975**, *1*, 2.

(15) For spectroscopic evidence pertaining to other arene–Hg(II) complexes based on ^1H and ^{13}C NMR shifts, see: (a) Olah, G. A.; Yu, S. H.; Parker, D. G. *J. Org. Chem.* **1976**, *41*, 1983. (b) Damude, L. C.; Dean, P. A. W. *J. Organomet. Chem.* **1979**, *181*, 1.

(16) For evidence relating to the facile rotation of arene rings in crystalline complexes, see: Fyfe, C. A.; Harold-Smith, D.; Ripmeester, J. *J. Chem. Soc., Faraday Trans. 2* **1976**, *72*, 2269 [for leading references].

(17) For a similar comparison of arene–$Hg(SbF_6)_2$ complexes, see: Damude, L. C.; Dean, P. A. W.; Sefcik, M. D.; Schaefer, J. *J. Organomet. Chem.* **1982**, *226*, 105.

(18) For previous NMR evidence of a 1:1 complex of HMB and HgT_2, see Damude and Dean in ref 15b.

(19) Benesi, H. A.; Hildebrand, J. H. *J. Am. Chem. Soc.* **1949**, *71*, 2703. Person, W. B. *Ibid.* **1965**, *87*, 167.

indicate that the EDA complex is ~15 times more stable in trifluoroacetic acid than in dichloromethane. Otherwise the properties of the [HMB,HgT_2] complex are not strongly differentiated in these structurally different solvents. Furthermore the accuracy of the data is not sufficient to distinguish the formation of a 1:1 complex in solution from the 1:1 dimeric structure of the crystalline complex in Figure 1.

Photoproducts and Stoichiometry of the CT Irradiation of the [HMB,HgT_2] Complex. The EDA complex of hexamethylbenzene and mercuric trifluoroacetate was irradiated in dichloromethane and in trifluoroacetic acid with light filtered at 360 ± 20 nm. This light corresponds to the low energy tail of the CT band (see Figure 1) and thus ensures that there is no adventitious excitation of either the uncomplexed donor (HMB) or the acceptor (HgT_2).

When the CT irradiation of the EDA complex was carried out in dichloromethane as solvent, pentamethylbenzyl trifluoroacetate was formed as the exclusive organic product according to the stoichiometry in eq 3. The

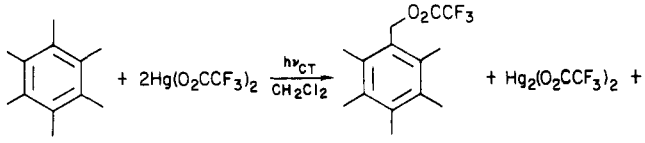

(3)

mercurous acetate crystallized from solution as colorless needlelike crystals. It was identified by elemental analysis and confirmed by comparison of the infrared spectrum with that of authentic sample.[20]

When the CT irradiation of the EDA complex was carried out in trifluoroacetic acid as solvent, pentamethylbenzyl acetate was again the sole organic product. However, the mercury-containing product in this solvent consisted of a mass of gray solid which cleanly afforded a globule of metallic mercury when washed with aqueous perchloric acid. The weight of the mercury globule together with the quantitative analysis of the benzylic ester indicated the stoichiometry in trifluoroacetic acid to be that shown in eq 4.

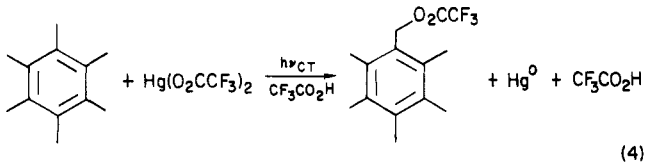

(4)

No thermal reaction could be detected between HMB and HgT_2 in either dichloromethane or trifluoroacetic acid, even upon prolonged heating of the solutions. In both solvents, the photochemical conversion of hexamethylbenzene could be driven almost to completion by prolonged irradiation. Despite those extreme conditions, no other byproducts were observed, and the side chain substitution of hexamethylbenzene proceeded according to eq 3 and 4.

Quantum Yields for the CT Photochemistry of the [HMB,HgT_2] Complex. The quantum yield for product formation from the CT photochemistry was determined by ferrioxalate actinometry under an argon atmosphere. The determination of the benzylic ester by quantitative gas chromatography using the internal standard method was performed on solutions in which the photolysis were carried out to 20–30% conversion. Although the analytical precision in detecting small changes was somewhat limited,

(20) (a) Swarts, F. *Bull. Soc. Chim. Belg.* **1939**, *48*, 176. (b) Sikirica, M.; Gredenic, D. *Acta Crystallogr., Sect. B* **1974**, *B30*, 144.

Table I. Photochemical Conversion of the [HMB,HgT_2] Complex in Trifluoroacetic Acid[a]

irradiation, s	additive,[b] vol %	hexamethylbenzene final	μmol consumed	ester,[c] μmol
40		15.4	4.6	3.7
20	5	15.5	4.5	4.0
40	5	13.7	6.3	5.6
20	50	15.0	5.0	3.8
40	50	11.5	8.5	8.5
40		14.8	5.2	4.1
40	50	11.7	8.3	8.1
40	50	11.4	8.6	7.9
20		16.8	3.2	2.3
40		14.5	5.5	4.9
20		16.5	3.5	3.3
30		15.2	4.8	5.0
40		14.5	5.5	7.1
60		11.9	8.1	8.0
20	5	15.2	4.8	3.9
30	5	14.1	5.9	6.7
40		14.2	5.8	3.6
20		14.9	5.1	5.9
10	5	15.4	4.6	4.4
20	5	14.8	5.2	5.5
30	5	14.4	5.6	5.7
10	5	16.1	3.9	3.9
20	5[d]	15.1	4.9	4.5
20	*d*	15.0	5.0	5.6

[a] In 2 mL trifluoroacetic acid solution containing 20 μmol of HMB and HgT_2 irradiated at 400 > λ > 300 nm and 20 °C. [b] Added trifluoroacetic anhydride. [c] Pentamethylbenzyl trifluoroacetate formed. [d] Contains 0.01 M lithium trifluoroacetate.

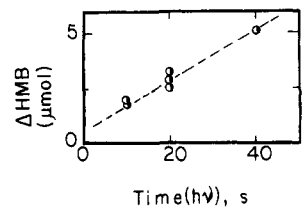

Figure 4. Photochemical conversion of HMB from the CT irradiation of 1×10^{-2} M HMB and HgT_2 in trifluoroacetic acid at 20 °C after a standard 1-min aqueous quench.

the product quantum yield Φ_P could be measured reproducibly to within ±0.1. At low conversions, the quantum yield was monitored continuously by following the absorbance change ΔA_{CT} of the CT band (vide supra).

In dichloromethane solution, the quantum yield for the CT photochemistry of the [HMB,HgT_2] complex was readily and reproducibly measured to be essentially unity (i.e., $\Phi_P = 0.9 \pm 0.1$). In strong contrast, the value of Φ_P in trifluoroacetic acid varied from ~2 to 3, under otherwise identical conditions. Furthermore the results summarized in Table I reveal an unusually large amount of scatter in the data. In order to develop reproducible conditions for the CT irradiation, a series of identical samples were subjected to the standard photochemical conditions listed in Table II. We found that it was most important to maintain consistency in the time elapsed prior to quenching the reaction in order to obtain the reproducibility shown in Figure 4. Even under these optimum conditions, the experimental scatter exceeded the variation in the light intensity (see Experimental Section). The dashed line represents a unit quantum yield as measured with a constant light source (400 > λ > 300 nm).

The origin of the apparent irreproducibility was traced in the following way to the participation of a thermal process which continued in the dark after the light was turned off. This postreaction was established by continually measuring the change in the intensity of the CT

Table II. Reproducibility Check on the Photochemical Conversion of the [HMB,HgT_2] Complex in Trifluoroacetic Acid[a]

irradiation, s	Additive,[b] vol %	quench,[c] min	hexamenthylbenzene[d] final	hexamenthylbenzene[d] consumed
10		1	18.2	1.8
10		5	17.1	2.9
10	5	1	18.0	2.0
10	5	5	16.4	3.6
20		1	17.6	2.4
20		5	16.0	4.0
20	5	1	16.8	3.2
20	5	5	16.0	4.0
40		1	14.9	5.1
20		1	17.1	2.9
20	5	1	16.7	3.3

[a] In 2 mL of trifluoroacetic acid solution containing 20 μmol of HMB and HgT_2 irradiated at 400 > λ > 300 nm and 20 °C. [b] Added trifluoroacetic anhydride. [c] Interval at which aqueous quench initiated. [d] μmol.

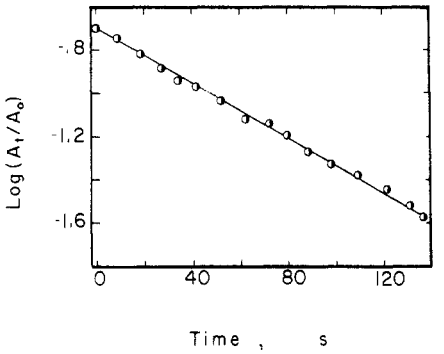

Figure 5. The decay of the CT absorption band at λ 390 nm following the 360-nm irradiation of 1×10^{-2} M HMB and HgT_2 in trifluoroacetic acid at 25 °C, plotted as the logarithm of the CT absorbance minus background with time.

absorption band of the [HMB,HgT_2] complex during and after exposure to light. As expected, during irradiation the CT absorbance of the EDA complex decreased linearly by an amount ΔA_{CT} with irradiation time (Δt) at low conversions. When was surprising, however, was that the CT absorbance continued to decrease by an additional amount δA_{CT} after the light was shuttered, as shown in Figure 5. This postreaction serves to magnify the photochemical effect. Indeed the results in Table III (entry 1) indicate that for Δt = 10 s, the apparent quantum yield is 4 times larger than the real quantum yield [i.e., $(\Delta A_{CT} + \delta A_{CT})/\Delta A_{CT} = 4$] as a result of the additional dark reaction. Since the incremental change (δA_{CT}) appears to be rather constant, the apparent discrepancy in the quantum yields decreases with increasing conversion (i.e., ΔA_{CT}).

The occurrence of the postreaction can thus account for the high, variable quantum yields in Table I and Figure 3.[21] The effects of such a dark process are also manifested in the marked temperature dependence of the quantum yield. Thus a decrease in temperature from +20 to −20 °C led to a ~50-fold decrease in the quantum yield, as monitored by the change in the CT absorbance in Table IV. A further decrease in temperature to −32 °C effected a 100-fold decrease in the quantum efficiency with which the [HMB,HgT_2] complex is consumed. By the same token, increasing the reaction temperature would lead to enhanced values of the observed quantum yields.

(21) The exact timing of the irradiation and the quench are difficult to control.

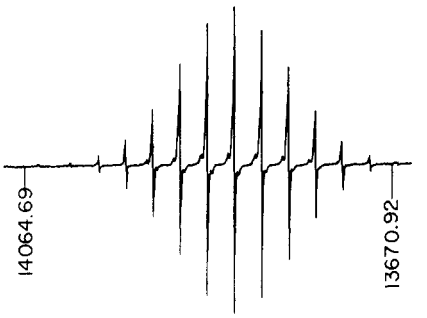

Figure 6. ESR spectrum obtained from the irradiation of the CT absorption band of the 1:1 EDA complex of HMB and HgT_2 in trifluoroacetic acid solution at 25 °C. The proton NMR field markers are in kHz.

Kinetics of the Postreaction of the [HMB,HgT_2] Complex. In order to examine the nature of the postreaction, we monitored the absorbance change ΔA_{CT} immediately following the interruption of radiation. The rate profile shown in Figure 5 indicates that the postreaction follows a first-order decay. The reproducibility of the first-order rate constant in trifluoroacetic acid and in trifluoroacetic acid containing trifluoroacetic anhydride is shown by the results in Table V.

ESR Spectra of Transient Intermediates from the CT Excitation. A solution of 5.6×10^{-3} M hexamethylbenzene and 7.2×10^{-3} M mercuric trifluoroacetate was irradiated at the CT absorption band directly in the cavity of the ESR spectrometer. The well-resolved ESR spectrum in Figure 6 obtained in trifluoroacetic acid at 25 °C consisted of at least 15 lines with hyperfine splitting a_H = 6.5 G and $\langle g \rangle$ = 2.0024. This spectrum is the same as that of the hexamethylbenzene cation–radical generated independently[22]—the relative intensities of the lines being in accord with the binomial ratios for 18 equivalent protons. Indeed at higher gain, the increased signal amplitude reveals the presence of the additional wing lines of the would-be 19-line pattern.

When a solution of 7.9×10^{-3} M hexamethylbenzene and 11.4×10^{-3} M mercuric trifluoroacetate was irradiated at 25 °C in dichloromethane under equivalent conditions, the same ESR spectrum was obtained as that shown in Figure 6—but with significantly diminished amplitude. Irradiation at −60 °C afforded a broadened ESR spectrum with at least 13 lines with a_H = 6.5 G and $\langle g \rangle$ = 2.0023 shown in Figure 7a. The broad lines were resolved at −100 °C to a complex ESR spectrum shown in Figure 7b. This spectrum was computer simulated successfully by the superposition in Figure 7b′ of a pair of component spectra shown in Figure 7a′,a″. The latter were derived from the binomial simulation of (Figure 7a′) the 19-line pattern with a_H = 6.5 G on the left and (Figure 7a″) the 37-line pattern with a_H = 3.1 G on the right. [The composite spectrum in Figure 7b′ was generated by their combination in a 85:100 intensity ratio.] The 37-line spectrum is readily assigned to the cation-radical of the π-dimer of hexamethylbenzene.[23,24]

The same experimental ESR spectra (Figure 7) consisting of these two components was also observed in trifluoroacetic acid when a large excess of hexamethyl-

(22) (a) Elson, I. H.; Kochi, J. K. *J. Am. Chem. Soc.* **1973**, *95*, 5061. (b) Schlesener, C. J.; Amatore, C.; Kochi, J. K. *Ibid.* **1984**, *106*, 3567. (c) Schlesener, C. J.; Amatore, C.; Kochi, J. K. *Ibid.* **1984**, *106*, 7472.

(23) (a) Edlund, O.; Kinell, P.-O.; Lund, A.; Shimizu, *J. Chem. Phys.* **1967**, *46*, 3679. (b) Badger, B.; Brocklehurst, B. *Trans. Faraday Soc.* **1969**, *65*, 2582, 2588.

(24) See also: Kira, A.; Arai, S.; Iwamura, M. *J. Phys. Chem.* **1972**, *76*, 1119.

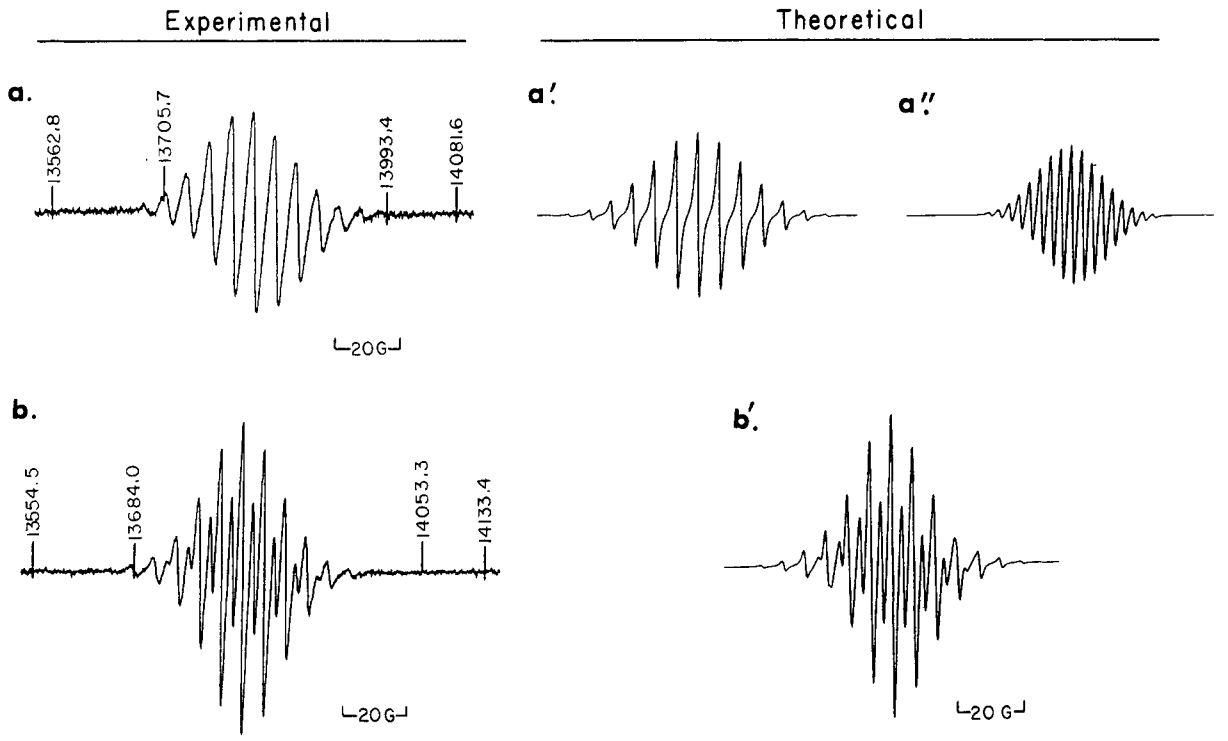

Figure 7. (a) ESR spectra obtained from the irradiation of the [HMB,HgT_2] complex in dichloromethane at (a) −60 °C and (b) −100 °C. Proton NMR field numbers are in kHz. Computer simulation (a′) of 18 equivalent protons with a_H = 6.5 G, (a″) of 36 equivalent protons with a_H = 3.1 G, (b′) superposition of a′ and a″ in 85:100 intensity ratio.

Table III. Experimental Demonstration of the Postreaction Following CT Irradiation of the [HMB,HgT_2] Complex in Trifluoroacetic Acid[a]

		absorbance (λ 390 nm)				
irradiation, s	additive,[b] vol %	initial	stop[c]	final[d]	ΔA_{CT}	δA_{CT}
10		2.23	2.13	1.81	0.10	0.32
10	5	2.06	1.90	1.62	0.16	0.28
20		2.22	1.97	1.69	0.25	0.28
20	5	2.08	1.81	1.53	0.27	0.28
60		2.18	1.42	1.18	0.76	0.24

[a] In 2 mL of trifluoroacetic acid solution containing 1.0 × 10^{-2} M HMB and HgT_2 at 20 °C. [b] Added trifluoroacetic anhydride. [c] After interruption of irradiation. [d] 5 min later.

Table IV. Temperature Dependence on the CT Photochemistry of the Following Complex in Trifluoroacetic Acid[a]

			hexamethylbenzene[c]			
temp, °C	irradiation, s	additive,[b] vol %	final	reacted	ester,[d] μmol	Φ_P
−19	300	50	17.9	2.1	1.4	0.05
−19	300		16.8	3.2	2.6	0.07
−32	600	50	18.2	1.8	1.0	0.02
20	60		13.3	6.7	7.1	
20	60		16.4[e]	3.6[e]	3.0[f]	

[a] In 2 mL of trifluoroacetic acid solution containing 20 μmol of HMB and HgT_2. [b] Added trifluoroacetic anhydride. [c] μmol. [d] Pentamethylbenzyl trifluoroacetate. [e] HMB-d_{18}. [f] Perdeuterio derivative.

Table V. Postreaction. The Decay of the CT Absorbance Following the Irradiation of the [HMB,HgT_2] Complex in Trifluoroacetic Acid[a]

		absorbance (390 nm)			
additive,[b] vol %	irradiation, s	initial	stop[c]	final[d]	k_{obsd},[e] $10^2 s^{-1}$
	20	2.22	1.97	1.69	1.1
	20	2.21	1.93	1.56	1.4
5	20	1.97	1.73	1.48	1.0
5	20	2.08	1.81	1.53	1.0
	10	2.23	2.13	1.81	0.7
5	10	2.06	1.90	1.62	1.4

[a] In 2 mL of trifluoroacetic and solution containing 20 μmol of HMB and HgT_2 at 20 °C. [b] Added trifluoroacetic anhydride. [c] Immediately after radiation interrupted. [d] After 5 min. [e] From the decay of the CT absorbance (cf. Figure 5).

benzene was present. Thus the irradiation of 2.1 × 10^{-2} M HMB and 3.9 × 10^{-3} M HgT_2 in trifluoroacetic acid resulted in the broadened ESR spectrum (cf. Figure 7a), and it resolved into the two overlapping patterns (cf. Figure 7b) at −40 °C. All attempts to observe the ^{199}Hg splittings for a mercury(I) species were unsuccessful.[25]

Kinetics of the Disappearance of the Hexamethylbenzene Cation-Radical Intermediate. The

(25) From the reports of mercury(I) radicals trapped in solid matrices [see: Booth, R. J.; Starkic, H. C.; Symons, M. C. R. *J. Chem. Soc. A* **1971**, 3198. Symons, M. C. R.; Yandell, J. K. *Ibid.* 1971, 760], we surmise that such species may be unobservable under experimental conditions.

(26) For our purposes here, it was not mandatory to establish the exact kinetics order of the decay—only that it was at least biphasic.

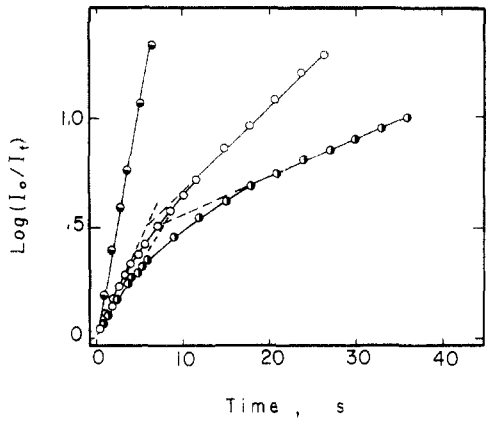

Figure 8. The decay of the hexamethylbenzene cation–radical following the irradiation of (◒) 2.5×10^{-3}, (○) 2×10^{-2}, and (◑) 5×10^{-2} M HMB and HgT_2 in trifluoroacetic acid at 20 °C.

Table VI. First-Order Rate Constants for the Decay of $HMB^{+}\cdot$ Following CT Irradiation of the [HMB,HgT_2] Complex in Trifluoroacetic Acid[a]

HMB, M	HgT_2, M	k, s^{-1} A	k, s^{-1} B
0.0025	0.0025	0.48	
0.02	0.02	0.20	0.087
0.05	0.05	0.15	0.039
0.0025	0.0025[b]	0.11	0.071
0.05	0.05[b]	0.13	0.025
0.02	0.02[c]	0.21	0.012

[a] In 2 mL of trifluoroacetic acid at 25 °C. [b] HMB-d_{18}. [c] Contains 0.1 M lithium trifluoroacetate.

ESR spectrum of hexamethylbenzene cation–radical diminished rapidly once the light was turned off. The changes in the concentration of the radical–cation was monitored by observing the amplitude of one of the central lines of the ESR spectrum. Thus the signal intensity of the cation–radical reached a maximum (steady-state condition) within a few seconds after an equimolar solution of HMB and HgT_2 in trifluoroacetic acid was exposed to the light. Upon shuttering the light, the signal decayed immediately, and it was completely gone within a minute. Typical decay profiles are shown in Figure 8 in which the ratios of the initial signal intensity I_0 to that (I_t) at time t are plotted logarithmically. Clearly the rate profile of the cation–radical is highly concentration dependent. At very low concentrations of HMB and HgT_2 (2.5×10^{-3} M), the decay of the cation–radical follows first-order kinetics throughout.

At higher concentrations (2.0×10^{-2} M), the rate profile show biphasic behavior which we assign to two concurrent first-order processes A and B.[26] It is noteworthy that the rates of both A and B are slower than that (A) observed at the lower concentration. The differentiation between the two processes (i.e., A/B), together with the diminution in their absolute rates, is even more pronounced at higher concentrations (5.0×10^{-2} M). An estimate of these rate processes are included in Table VI as first-order rate constants.

The presence of added lithium trifluoroacetate as a common ion had only a slight effect on process B and almost no effect on process A.

The pronounced kinetic isotope effect on the decay of the cation–radical is illustrated in Figure 9 with hexamethylbenzene-d_{18}. At the lowest concentration (2.5×10^{-3} M), the first-order decay observed with HMB is replaced by a much slower and less linear first-order decay with HMB-d_{18}. The latter is included in Table VI as two rate

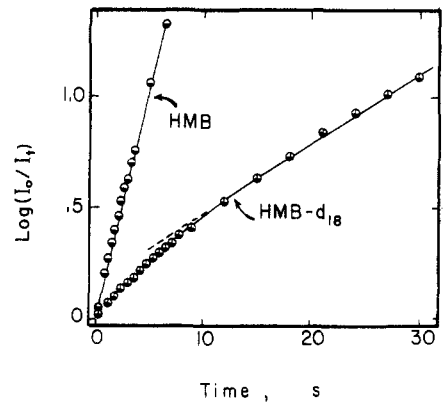

Figure 9. Kinetic isotope effect on the decay of $HMB^{+}\cdot$ following the CT irradiation of the EDA complex derived from 2.5×10^{-3} M (◒) $(CH_3)_6C_6$ or (●) $(CD_3)_6C_6$ and 2.5×10^{-3} M HgT_2 in trifluoroacetic acid at 25 °C.

constants. The kinetic isotope effects for processes A and B are significantly attenuated at the higher concentrations (5.0×10^{-2} M).

Discussion

The formation of the π-complex of hexamethylbenzene and mercuric trifluoroacetate is demonstrated by the crystal structure shown in Figure 2. The comparison of the spectral properties (UV–vis, ^1H and ^{13}C NMR) of the crystalline complex with the EDA complex in solution establishes the essential charge-transfer (CT) nature of the optical transition in both as arising from the 1:1 interaction of mercury(II) with the aromatic donor. Thus a slight uncertainty as to whether the dimeric structure persists in solution is not of concern here. For expediency, we proceed with the formulation of the EDA complex simply as [HMB,HgT_2] in solution.

The attendant charge-transfer photochemistry of the [HMB,HgT_2] complex merits attention for two reasons. First, the quantum yield Φ_p for product formation is (a) large and can be >1, (b) highly solvent dependent, and (c) strongly temperature dependent. Second, the stoichiometry of the photoreaction is cleanly differentiated in dichloromethane from that in trifluoroacetic acid, as represented in eq 3 and 4, respectively. The striking difference lies in the nature of the reduced mercury-containing product consisting of either mercurous trifluoroacetate or metallic mercury. The oxidized pentamethylbenzyl trifluoroacetate is the sole organic product in both solvents.

Any mechanistic formulation of this unusual photochemistry must accomodate these diverse observations. We begin by noting that both the ESR and visible absorption spectra of the transient hexamethylbenzene cation–radical are observed immediately upon the irradiation of the charge-transfer band of the [HMB,HgT_2] complex. The deliberate use of the filtered light with λ = 360 nm ensures that such a spectral transient does not arise from the adventitious excitation of either the free donor HMB or the free acceptor HgT_2. The observation of $HMB^{+}\cdot$ is a direct consequence of the charge-transfer excitations of the EDA complex according to Mulliken theory,[9,10] i.e., eq 5. As such, $HMB^{+}\cdot$ is the key reactive

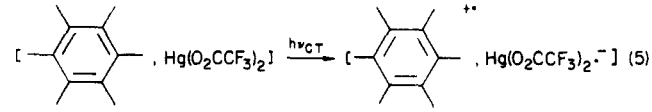

intermediate leading to the photoproduct pentamethylbenzyl trifluoroacetate in both dichloromethane and trifluoroacetic acid. Accordingly the collapse of the ion pair

following CT excitation in eq 5 represents an economical route to this benzylic ester, i.e., eq 6. Such a direct process

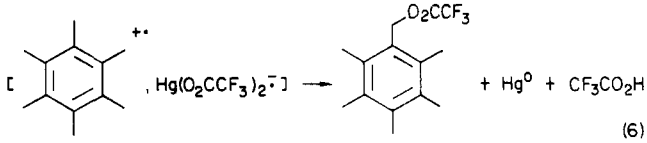

(6)

however cannot accommodate the observed quantum yield in excess of one, as listed in Table I. Moreover there are other reasons to suspect that the ion pair formed in eq 5 is too short-lived to participate in such a complex transformation. For example, the relative values of the redox potentials E^0 for HMB and HgT_2, indicate that the driving force for back electron transfer is sufficiently large to drive such an ion pair back to the reactants in <50 ps.[27] However, the decay of $HMB^{+}\cdot$ in Table VI clearly occurs on a time scale which is many orders of magnitude slower than this cage process. Accordingly, we assign the ESR spectra in Figures 6 and 7 to "free" $HMB^{+}\cdot$ rather than to an ion paired species. The latter is also indicated by the line width of the ESR spectrum in Figure 6 which shows no evidence of modulation by a paramagnetic counterion.[28] In other words the high experimental quantum yields and the ESR observation of relatively long-lived $HMB^{+}\cdot$ indicate that back electron transfer from the CT ion pair is not an important limitation. In order to account for the apparent inconsistency between the expected fast rate of back electron transfer of eq 5 and the observed lifetime of $HMB^{+}\cdot$, we suggest that the mercurous moiety $Hg(O_2CCF_3)_2^{-}\cdot$ is kinetically unstable and undergoes rapid ligand dissociation.[29] According to this formulation, the CT excitation is tantamount to a dissociative process, i.e., eq 7, which effectively retards the back electron transfer.[30]

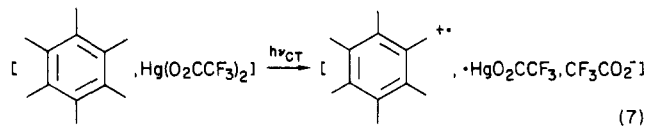

(7)

Consequently the diffusive separation of $HMB^{+}\cdot$ from the ion pair state will allow it to interact with a free HMB in solution to form the π-dimer cation–radical, i.e., eq 8, the

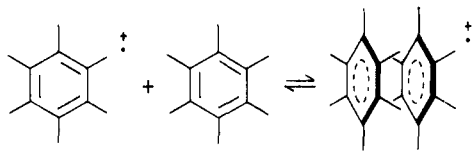

(8)

ESR spectrum of which is presented in Figure 7b. Although the formation constant of the dimer cation radical $(HMB)_2^{+}\cdot$ has not been measured, the ESR line broadening in Figure 7a suggests that eq 8 is a mobile equilibrium. Indeed the biphasic behavior of the ESR decay kinetics in Figures 8 and 9 is consistent with these two types of hexamethylbenzene cation–radicals.

The route by which $HMB^{+}\cdot$ is subsequently converted to the benzylic ester has been previously shown to occur via a multistep sequence consisting of proton transfer, oxidation, and solvation,[32,33] i.e., eq 9–11.

$$(CH_3)_5C_6CH_3^{+}\cdot \xrightarrow{[-H^+]} (CH_3)_5C_6CH_2\cdot \quad (9)$$

$$(CH_3)_5C_6CH_2\cdot \xrightarrow{[-e]} (CH_3)_5C_6CH_2^{+} \quad (10)$$

$$(CH_3)_5C_6CH_2^{+} + CF_3CO_2H \rightarrow (CH_3)_5C_6CH_2O_2CCF_3 + H^{+} \quad (11)$$

The pathway by which the mercurous species derived in eq 7 is converted to the mercury-containing products is less certain. The observation of mercurous trifluoroacetate as the sole product in dichloromethane (eq 3) suggests a simple dimerization, i.e.,[34] eq 12. If so, the

$$2\cdot HgO_2CCF_3 \rightarrow Hg_2(O_2CCF_3)_2 \quad (12)$$

observed quantum yield of unity in this solvent indicates that the oxidant in eq 10 is mercuric trifluoroacetate, i.e.,[35] eq 13. The overall photochemistry in dichloromethane would then consist of the CT excitation in eq 7 followed

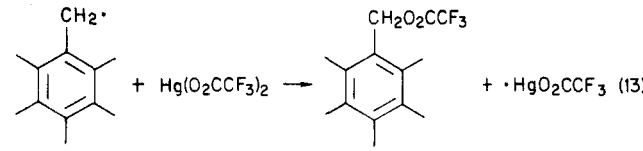

(13)

by diffusive separation of $HMB^{+}\cdot$ and proton loss in eq 9 and oxidation in eq 13. Dichloromethane as a relatively nonpolar, aprotic solvent would constitute the appropriate environment to promote the dimerization of the mercurous radical $\cdot HgO_2CCF_3$ in eq 12.

There are at least three potential pathways by which the mercurous radical is converted to metallic mercury in eq 4, viz., eq 14–16. The disproportionation of the mercurous radical in eq 14 does not account for values of the quantum

$$2\cdot HgO_2CCF_3 \rightarrow Hg(O_2CCF_3)_2 + Hg^0 \quad (14)$$

$$\cdot HgO_2CCF_3 \xrightarrow{[+e]} Hg^0 + CF_3CO_2^{-} \quad (15)$$

$$\cdot HgO_2CCF_3 \rightarrow Hg^0 + CF_3CO_2\cdot \rightarrow CO_2 + CF_3\cdot, \text{ etc.} \quad (16)$$

yield $\Phi_P > 1$ obtained in trifluoroacetic acid. Furthermore the homolytic fragmentation of the mercurous radical in eq 16 is unlikely since no carbon dioxide, perfluoroethane, or fluoroform (as expected from the ready decarboxylation of the trifluoroacetoxy radical[36]) is observed among the photolysis products. We are therefore left with the last

(27) (a) For example the lifetime of the CT ion pair from HMB and tetracyanoethylene (TCNE) is <50 ps.[8a] Since HgT_2 is likely to have a significantly larger E^0 than TCNE, the rate of back electron transfer should be even faster. [For the free energy relationship between the driving force and the rate of electron transfer, see: Klingler, R. J.; Kochi, J. K. *J. Am. Chem. Soc.* **1982**, *104*, 4186. See also ref 22b.] (b) At this juncture we are unable to evaluate the possibility that rapid intersystem crossing of the excited ion pair to a triplet state slows down back electron transfer (as possibly shown by CIDNP studies). Such a relaxation process does not fundamentally change the arguments presented herein.

(28) The linewidth of ~60 mG is similar to that in ref 22.

(29) This formulation accords with the irreversibility of the cathodic cyclic voltammogram of mercuric trifluoroacetate even at high sweep rates.

(30) For an analogous reasoning in the CT photochemistry of the EDA complexes of tetranitromethane, see ref 8b,c.

(31) We differentiate this broadening from that due to the mercurous radical.[29]

(32) (a) Svanholm, U.; Parker, V. D. *Tetrahedron Lett.* **1972**, 471. (b) Dessau, R. M.; Shih, S.; Heiba, E. I. *J. Am. Chem. Soc.* **1970**, *92*, 412. (c) Wagner, P. J.; Lam, H. M. H. *Ibid.* **1980**, *102*, 4167. (d) It is possible that deprotonation also occurs from the dimer cation radical, albeit at a slower rate.

(33) For useful reviews of chemical and electrochemical methods for the oxidative transformations of methylarenes to benzylic esters by successive one-electron transfer, see: (a) Littler, J. S.; Nonhebel, D. C. *Int. Rev. Sci. Org. Chem., Ser. 2* **1975**, *10*, 211–275. (b) Chambers, J. Q. *Ibid.* **1975**, *10*, 317–355. (c) Yoshida, K. *Electroxidation in Organic Chemistry*; Wiley: New York, 1984.

(34) We cannot evaluate the possibility that the formation of $Hg_2(O_2CCF_3)_2$ is a cage process which derives from the dimeric structure in Figure 2 persisting in solution.

(35) The oxidation of the benzyl radical is facile. [See: Rollick, K.; Kochi, J. K. *J. Am. Chem. Soc.* **1982**, *184*, 1319.] Furthermore there is no evidence in the ESR studies for the benzylic radical.

(36) Cf.: May, D. D.; Skell, P. S. *J. Am. Chem. Soc.* **1982**, *104*, 4500.

alternative in eq 15 that the mercurous radical is an oxidant. Although such a conclusion may on first sight seem to be unreasonable, the postulate does provide a ready explanation of two otherwise unexplicable observations, viz., quantum yields that can be as high as 3 and the chain propagation of the dark reaction. For example, the oxidation of hexamethylbenzene by mercurous trifluoroacetate in eq 17 would formally represent one homolytic

$$(CH_3)_5C_6CH_3 + \cdot HgO_2CCF_3 \rightarrow (CH_3)_5C_6CH_2\cdot + Hg^0 + CF_3CO_2H \quad (17)$$

step of a chain reaction. Eq 17 followed by eq 13 constitute the propagation cycle for the overall thermal process in eq 18. The benzylic ester and metallic mercury produced

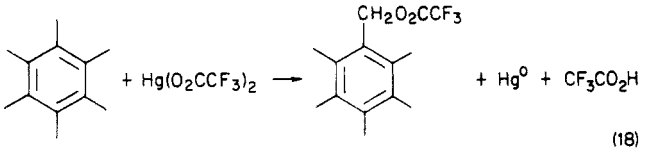

(18)

in eq 18 is the thermal counterpart to that derived from the CT photochemistry in eq 4. Conceptually the radical-chain process leading to eq 18 via eq 17 and 13 could lead to quantum yields far in excess of one. The experimental values of ~2–3 indicate a rather short kinetic chain length, undoubtedly arising from the inefficiency of eq 17.

Generalized Mechanism for CT Photochemistry. All of the diverse experimental observations for the CT photochemistry of the [HMB,HgT_2] complex in dichloromethane and trifluoroacetic acid can be accommodated within a single framework based on the initial process associated with the photoactivation shown in Scheme I.

Scheme I

$$HMB + HgT_2 \rightleftharpoons [HMB,HgT_2] \quad (19)$$

$$[HMB,HgT_2] \xrightarrow{h\nu_{CT}} [HMB^+\cdot,HgT_2^-\cdot] \quad (20)$$

$$[HMB^+\cdot,HgT_2^-\cdot] \xrightarrow{<50ps} [HMB^+\cdot,HgT\cdot,T^-] \quad (21)$$

$$[HMB^+,HgT\cdot,T^-] \xrightarrow{diffuse} HMB^+ + HgT\cdot + T^- \quad (22)$$

In essence, this series of fast reactions serve to produce a pair of separated reactive species $HMB^+\cdot$ and ·HgT, which is unable to suffer back electron transfer. Thus the pair of radicals must undergo thermal reactions which we present as Schemes II and III.

Scheme II

$$HMB^+\cdot + CF_3CO_2^- \rightarrow (CH_3)_5C_6CH_2\cdot + CF_3CO_2H \quad (23)$$

$$(CH_3)_5C_6CH_2\cdot + HgT_2 \rightarrow (CH_3)_5C_6CH_2O_2CCF_3 + \cdot HgT \quad (24)$$

$$HMB^+\cdot + HMB \rightleftharpoons (HMB)_2^+\cdot \quad (25)$$

Scheme III

$$\cdot HgT + HMB \rightarrow Hg^0 + (CH_3)_5C_6CH_2\cdot + CF_3CO_2H \quad (26)$$

$$\cdot HgT + \cdot HgT \rightarrow Hg_2T_2 \quad (27)$$

According to Scheme II, the fate of the aromatic cation radical $HMB^+\cdot$ is relatively straightforward. The deprotonation of $HMB^+\cdot$ is known to be a relatively slow process,[22c] and the observed kinetic isotope effect of ~4 (Table VI) is consistent with this route to the pentamethylbenzyl radical. The rapid subsequent oxidation of the latter with HgT_2 (eq 24) proceeds via the benzylic cation, in accord with the isotopic deuterium incorporation from the solvent. (See the Experimental Section.) The formation of the π-dimer cation radical $(HMB)_2^+\cdot$ in eq 25 is shown by its ESR spectrum in Figure 7b. The enhanced stability of the dimeric species as noted by the diminished rate of disappearance (especially at relatively high concentrations of HMB) is consistent with the extensive electron delocalization in this extended π-system.[37] The marked dependence of the kinetic isotope effect on the concentration of HMB is consistent with the reversibility of eq 25. At low concentrations of HMB, the rate (Figure 9) and kinetic isotope effect (Table VI) are determined by process A for [$HMB^+\cdot$] owing to the minor concentrations of $(HMB)_2^+\cdot$. At high concentrations of HMB, the rate and the kinetic isotope effect are limited by the prodominance of process B for $[HMB]_2^+\cdot$ since the reversion to $HMB^+\cdot$ and not deprotonation will constitute the slow, rate-determining process.

According to Scheme III, the fate of the mercurous trifluoroacetate radical ·HgT is largely controlled by the solvent. In an aprotic, nonpolar medium such as dichloromethane, ·HgT is subject to rapid dimerization. However in the protic trifluoroacetic acid, possibly due to enhanced solvation, the mercurous radical is sufficiently longer liver to oxidize HMB (eq 26). Such a thermal oxidation of a second equivalent of hexamethylbenzene can be a relatively slow process as judged by the rather prolonged period of the postreaction. If the oxidation in eq 26 proceeds via $HMB^+\cdot$, the mercurous radical is not expected to be a powerful outer-sphere oxidant. Indeed it is plausible for the oxidation of HMB to occur via an alternative route involving hydrogen atom transfer, i.e., eq 28 and 29. Such a hydrogen abstraction is the microscopic reverse of a homolytic process which was proposed earlier.[38,39] It is consistent with the observation that the post reaction sustains itself for 3–5 min after irradiation (Figure 5 and Table V), whereas the decay of $HMB^+\cdot$ observed by its ESR spectrum (Figure 8 and Table VI) is complete with a minute. The strong dependence of the quantum yield Φ_P on the temperature can be accommodated by the low reactivity of the mercurous radical and/or its reversible anation which favors $HgT_2^-\cdot$ sufficient to facilitate back electron transfer of eq 5. However, the presence of lithium trifluoroacetate did not appear to have

$$(CH_3)_5C_6CH_3 + \cdot HgO_2CCF_3 \rightarrow (CH_3)_5C_6CH_2\cdot + H{-}HgO_2CCF_3 \quad (28)$$

$$H{-}HgO_2CCF_3 \rightarrow Hg^0 + CF_3CO_2H \quad (29)$$

(37) Note the equivalence of 36 protons with ^1H hfs of one-half that of $HMB^+\cdot$ indicates complete electron delocalization between the two benzenoid moieties in $(HMB)_2^+\cdot$.

(38) (a) Gray, G. A.; Jackson, W. R.; Chambers, V. M. A. *J. Chem. Soc. C* **1971**, 200. (b) Chambers, V. M. A.; Jackson, W. R.; Young, G. W. *J. Chem. Soc., Chem. Commun.* **1970**, 1275. (c) Whitesides, G. M.; San Filippo, J., Jr. *J. Am. Chem. Soc.* **1970**, *92*, 6611. These studies present homolytic hydrogen transfer from a putative alkylmercury(II) hydride to generate an alkylmercurous radical. However this radical should have different redox properties from a trifluoroacetomercury radical proposed in this study.[39]

(39) (a) It is important to emphasize that the redox properties of a metal-centered radical or complex is highly dependent on the ligand. For example $Hg(O_2CCF_3)_2$, $Tl(O_2CCF_3)_3$, and $Pb(O_2CCF_3)_4$ are well-known oxidants whereas the corresponding alkyls $Hg(CH_3)_2$, $Tl(CH_3)_3$, and $Pb(CH_3)_4$, respectively, are reducing agents.[40] (b) Preliminary studies indicate that the CT irradiation of the EDA complex of HMB and mercurous trifluoroacetate with λ_{max} = 311 nm also produces pentamethylbenzyl trifluoroacetate and metallic mercury in accord with the stoichiometry

$$(CH_3)_5C_6CH_3 + Hg_2(O_2CCF_3)_2 \xrightarrow{h\nu_{CT}} (CH_3)_5C_6CH_2O_2CCF_3 + 2Hg^0 + CF_3CO_2H$$

(40) See: Kochi, J. K. *Organometallic Mechanisms and Catalysis*; Academic: New York, 1978.

a significant dampening effect on the quantum yield.[41]

Experimental Section

Materials. The aromatic hydrocarbons were obtained from commercial sources and repurified as follows. Hexamethylbenzene, pentamethylbenzene, and durene (Aldrich Chemical Co.) were recrystallized from ethanol and sublimed. Prehnitene and mesitylene (Aldrich) were refluxed over sodium and distilled under reduced pressure. The isomeric purity of each hydrocarbon was established by gas chromatographic analysis on a Hewlett-Packard 5790 chromatograph equipped with a 12-m capillary column coated with cross-linked methylsilicone. Hexamethylbenzene-d_{18} (Merck) was received as a gift from Dr. R. A. Nader (Du Pont) and used as such.

Mercuric trifluoroacetate $Hg(O_2CCF_3)_2$, prepared from mercuric oxide and trifluoroacetic acid, was recrystallized from a mixture of trifluoroacetic acid and trifluoroacetic anhydride. Trifluoroacetic acid (Halocarbon Products, Inc.) was refluxed over P_2O_5 and then distilled by taking only a middle cut. Reagent grade dichloromethane was washed several times with concentrated H_2SO_4, followed by 50% aqueous Na_2CO_3, dried over $CaCl_2$, and distilled from P_2O_5 under an argon atmosphere. It was stored in a Schlenk flask under argon in the dark. Trifluoroacetic anhydride was prepared from trifluoroacetic acid and P_2O_5. All transfers involving mercuric trifluoroacetate or trifluoroacetic acid were carried out with all-glass hypodermic syringes equipped with a platinum needle.

Measurement of the Charge-Transfer Absorption Spectra. Solutions of HgT_2 and arene were prepared in the absence of direct room light. The absorption spectra of the separate donor (HMB) and acceptor (HgT_2) at appropriate concentrations were first measured on either a Perkin-Elmer 552 or a Hewlett-Packard 8450A UV–vis spectrometer and found to be optically transparent beyond 290 nm. The CT absorption spectrum of the EDA complex was measured by mixing solutions of the donor and acceptor at the same concentrations. In a typical experiment, stock solutions of 0.02 M HgT_2 and 0.12 M HMB were prepared in dichloromethane. A 3-mL sample, containing a 1.5-mL aliquot of the HgT_2 solution and 0.25 mL of the HMB solution prepared by dilution with dichloromethane, was measured in a 1-cm quartz cuvette. For solutions containing various amounts of trifluoroacetic acid, a 10 vol % stock solution of trifluoroacetic acid in dichloromethane was used as the diluent. Absorption spectra were obtained at −40 °C with a quartz cuvette equipped with a Schlenk top.

The pale yellow color formed when solutions of HgT_2 and HMB in CH_2Cl_2 were mixed persisted over a period of several days at room temperature. The absorption spectrum of a solution containing 0.005 M of both HgT_2 and HMB showed a new absorption band with λ_{max} at 315 nm (Figure 1) with intense HMB absorption in the UV region. The addition of CF_3CO_2H to the solution greatly enhanced the absorption of the CT band and also caused a slight shift of λ_{max} toward the UV region. The absorption of the CT band increased linearly with the amount of CF_3CO_2H present. When CF_3CO_2H was used as the solvent, the λ_{max} was observed at 304 nm with the absorbance at least 15 times greater than that observed in CH_2Cl_2. The absorbance also increased linearly with the concentration of HMB. Several other solvents were examined including CH_3CN, diethyl ether, and 3-methyltetrahydrofuran, but no CT absorptions were observed.

Mercuric trifluoroacetate, being only slightly soluble in CH_2Cl_2 (saturated solution ~0.03 M at 25 °C), was found to be considerably more soluble in the presence of HMB. The same effect was observed with HMB which, being only slightly soluble in CF_3CO_2H, became considerably more soluble with HgT_2 present. These observations indicate that the EDA complex is more soluble than either HgT_2 alone in CH_2Cl_2 or HMB alone in CF_3CO_2H. The solubility of HgT_2 in CH_2Cl_2 was also found to increase considerably by the addition of only a few percent by volume of CF_3CO_2H.

The reflectance spectrum of crystalline [HMB,HgT_2] which was ground in the form of a fine powder showed a broad CT band centered at ~330 nm on a Cary 14 spectrometer equipped with a Model 1411 diffuse reflectance accessory. The CT spectrum of the crystalline complex suspended in a mineral oil mull was as described in the text.

Isolation and X-ray Crystallography of the EDA Complex. Mercuric trifluoroacetate (2.12 g, 4.97 mmol) and hexamethylbenzene (0.811 g, 5.00 mmol) were introduced into a 40-mL Schlenk flask equipped with a side arm containing a coarse glass frit. The vessel was evacuated and 20 mL of degassed trifluoroacetic acid introduced. The contents were shaken in the dark until a homogeneous yellow solution was obtained. The side arm was cooled to 0 °C and the solvent allowed to slowly distill over a period of 24 h. The pale yellow solid was removed and stored under argon in the dark. A small amount left open to air under room light showed no visible change over a period of several days.

The X-ray crystallography of the complex was carried out at −165 °C on a Picker four-circle goniostat equipped with a Furnas monochromator (HOG crystal). The Picker X-ray generator was interfaced to a TI 980 minicomputer with slo-syn stepping motors to drive angles. This diffractometer utilized for data collection was designed and constructed locally.[42] The structure was solved by direct methods (LSAM) and Fourier techniques. The final full-matrix least-squares refinement allowed all hydrogen atoms to vary isotropically and all other atoms to vary anisotropically. All hydrogens were located in a difference synthesis phased on the refined non-hydrogen atoms. Crystal data: empirical formula, $HgC_{16}O_4F_6H_{18}$; crystal dimension, 0.16 × 0.056 × 0.040 mm; space group, $P\bar{1}$; cell dimensions at −165 °C (36 reflections), a = 12.338 (0) Å, b = 9.984 (0) Å, c = 8.900 (0) Å; α = 79.86 (6)°, β = 107.10 (5)°, δ = 116.29 (6)°; Z (molecules per unit cell) = 1; calculated density, 2.139 g cm^{-3}; wavelength 0.71069 Å; molecular weight, 1177.79; linear absorption coefficient, 84.892 cm^{-1} (maximum 0.4690, minimum 0.5550); collection range, $5° < 2\theta < 50°$; scan width and speed, 2.0 + dispersion at 4.0° min^{-1}; total reflections collected, 4681; number of unique intensities, 4217; number with $F > 0$, 4013; number with $F > \sigma(F)$, 3885; number with $F > 2.33\sigma(F)$, 3713; final residuals $R(F)$ = 0.0445, $R_w(F)$ = 0.0339; goodness of fit for last cycle, 3.071; maximum $\Delta\sigma$ for last cycle, 0.05. A final difference Fourier synthesis contained a peak of 1.9 e Å^{-3} located 0.1 Å from the mercury atom, and all other peaks were 0.7 e Å^3 in intensity. The former peak is probably due to inaccuracies in the absorption coefficient. The final atom coordinates together with the bond distances, bond angles, and the anisotropic thermal parameters are included in the supplementary materials.

NMR Spectra of the [HMB,HgT_2] Complex. Previous studies have established the usefulness of NMR spectroscopy in complex formation.[6a,15] In this regard, ^{1}H NMR spectra were less informative owing to the small magnitude of the downfield shift in complexed HMB relative to free HMB.[15b] The ^{13}C NMR spectrum of the complex was obtained from a 1:1.5 mixture of HgT_2 and HMB and in trifluoroacetic acid with a Bruker HX 270 (67.9 MHz) spectrometer. For ^{13}C excitation, 90° pulses of 20 μs duration at 10-s intervals was optimum. A range of 200 ppm was used with dichloromethane internal standard set at 53.8 ppm. The quartets at ~117 and 161 ppm were assigned to the trifluoromethyl carbon and the carbonyl carbon, respectively, judging from the magnitude of the fluorine coupling. The absence of two different trifluoroacetate signals indicated that there is a fast exchange between the HgT_2 and CF_3CO_2H (eq 30). The chemical

$$Hg(O_2CCF_3)_2 + {}^*CF_3CO_2H \rightleftharpoons Hg(O_2CCF_3)(O_2C{}^*CF_3) + CF_3CO_2H \quad (30)$$

shifts of the arene carbon atoms are summarized in Table VII. Only one signal was observed for both the aromatic and methyl carbon atoms even in a combination where excess arene was present. This indicated a fast exchange process between the complex and the free arene under the experimental conditions (eq 31). A similar observation has been made in related systems.[15]

$$[HMB,HgT_2] + {}^*HMB \rightleftharpoons [HMB^*,HgT_2] + HMB \quad (31)$$

With the fast exchange process occurring, all the chemical shifts

(41) This may be due to the low formation constant for $HgT_2^{-\cdot}$ in trifluoroacetic acid.

(42) Lau, W.; Huffman, J. C.; Kochi, J. K. *Organometallics* **1982**, *1*, 155.

Table VII. ^{13}C NMR Chemical Shifts of Hexamethylbenzene upon Complexation with Mercuric Trifluoroacetate[a]

relative ratio[b]				chem shift		
HgT_2	HMB	solvent	% TFA[c]	C_1[d]	C_2[e]	Δppm (C_1)[f]
	1	CF_3CO_2H		134.1	16.8	
	1	CH_2Cl_2		131.7	16.5	
1.0	1.0	CH_2Cl_2		133.0	16.6	1.3
1.0	1.0	CH_2Cl_2	5	135.3	17.0	3.6
1.0	1.0	CH_2Cl_2	12	136.4	17.2	4.7
1.0	1.0	CH_2Cl_2	33	137.4	17.4	5.7
1.0	1.5	CH_2Cl_2		132.6	16.6	0.9
1.0	1.5	CH_2Cl_2	2	133.6	16.8	1.9
1.0	1.5	CH_2Cl_2	5	134.6	16.9	2.9
1.0	1.5	CH_2Cl_2	12	135.5	17.0	3.8
1.0	1.5	CH_2Cl_2	33	136.3	17.2	4.6
1.0	2.0	CH_2Cl_2		132.5	16.6	0.8
1.0	2.0	CH_2Cl_2	2	133.3	16.7	1.6
1.0	2.0	CH_2Cl_2	5	134.1	16.8	2.4
1.0	2.0	CH_2Cl_2	12	134.7	16.9	3.0
2.0	1.0	CH_2Cl_2		133.4	16.7	1.7
1.0	1.0	CF_3CO_2H		140.1	18.0	6.0
1.0	1.5	CF_3CO_2H		138.3	17.6	4.2
[HMB,HgT_2]$_2$[g]		CH_2Cl_2		133.3	16.7	1.6
[HMB,HgT_2]$_2$[h]		CH_2Cl_2	5	135.6	17.1	3.9
[HMB,HgT_2]$_2$[h]		solid		135.8	17.5	
HMB[h]		solid		132.3	17.4	

[a] All chemical shifts expressed in ppm with respect to CH_2Cl_2 set at 53.8 ppm. All spectra recorded at room temperature. [b] Relative ratio of $Hg(TFA)_2$ to HMB with final concentration between 0.05–0.10 M of each component. [c] Percentage by volume. [d] Aromatic carbon. [e] Methyl carbon. [f] Downfield shift of aromatic carbon with respect to free HMB in CH_2Cl_2, except for the complex in CF_3CO_2H which is expressed with respect to free HMB in CF_3CO_2H. [g] Crystalline complex isolated from CF_3CO_2H. [h] Solid-state ^{13}C NMR spectra kindly provided by Dr. J. S. Frye of Colorado State University.

observed represent averaged values. The complexation shifts (Δ ppm) of the aromatic carbon increase upon the addition of trifluoroacetic acid from 1.3 ppm with dichloromethane alone to 6.0 ppm in trifluoroacetic acid for a 1:1 combination of HgT_2 and HMB. The results support the results of the UV–vis absorption spectra in which the presence of trifluoroacetic acid increases the complex formation. The decrease in Δppm with the increase in HMB/HgT_2 ratio and vice versa within the same solvent combination showed the effect of free arene on the exchange averaged value. Low-temperature experiments (to −30 °C) failed to reveal the slowing up of the exchange process. [It was further complicated by precipitation of HgT_2.] Most importantly the spectrum of the crystalline complex isolated from CF_3CO_2H showed identical shifts and behavior when dissolved in CH_2Cl_2 as that obtained from a 1:1 combination of HgT_2 and HMB in either CH_2Cl_2 or 5 vol % CF_3CO_2H in CH_2Cl_2. The methyl carbon atom showed similar trends as that of the aromatic carbon atom, but the magnitude were too small to be of significance. The solid-state ^{13}C NMR of the complex also showed a downfield shift of 3.5 ppm relative to solid HMB, but only one type of aromatic carbon was observed. With regard to the localized η^2-bonding of the mercury to the arene shown by the crystal structure, the inequivalence of the aromatic carbons atoms is either less than 0.3 ppm or it is averaged by rotational motion in the solid state.

The ^{199}Hg spectra were examined on a Nicolet NT-360 spectrometer set at 64.525 MHz and a sweep width of ±40 kHz in 10′mm tubes using Me_2Hg as an internal standard. For ^{199}Hg excitation, a 90° pulse of 15 μs duration at 0.6-s intervals was optimum. The ^{199}Hg resonance was shown earlier to be extremely sensitive to the change in environment, ranging over 2000 ppm between neat $(C_6H_5CH_2CH_2)_2Hg$ to $Hg(NO_3)_2$ in 70% HNO_3.[43]

The effect of environment on the ^{199}Hg resonance can be seen in the shift of HgT_2 in trifluoroacetic acid and dichloromethane (Δ ppm = 172). Relative to HgT_2 in CH_2Cl_2, the complexation of HgT_2 with 1 equiv of HMB showed only a 8 ppm downfield shift, which is also very close to the sample of the isolated [HMB,HgT_2] in CH_2Cl_2 (Δppm = 13). The results in Table VIII are consistent with the low formation constant of complex in CH_2Cl_2. The addition of 5% CF_3CO_2H again reflected the increase in the complex formation causing a 93 ppm downfield shift. The fast equilibrium processes resulted in the observation of only one ^{199}Hg resonance due to exchange. All attempts to measure the

Table VIII. ^{199}Hg NMR Spectra of Mercuric Trifluoroacetic with Hexamethylbenzene in Solution[a]

sample	solvent	conc, M	−ΔHz	−Δppm
$Hg(CH_3)_2$		c	0	0
HgT_2	CF_3CO_2H	0.05	165 992	2567
HgT_2	CH_2Cl_2	0.05	154 902	2395
HgT_2	CH_2Cl_2	0.05	154 367	2387
HMB		0.05		
HgT_2	CH_2Cl_2	0.05[b]	154 063	2382
HgT_2 + HMB	CH_2Cl_2 (3 mL) + CF_3CO_2H (0.15 mL)	0.31	148 868	2302

[a] All frequencies and chemical shifts were expressed with respect to $(CH_3)_2Hg$ at 0 Hz and 0 ppm with 64.67 MHz spectrometer frequency. [b] Concentration based on monomer. [c] Neat.

^{199}Hg resonance in the solid state by CP magic-angle spinning were unsuccessful.[44]

ESR Spectra of Transient Intermediates in the CT Photochemistry. Solutions of the EDA complex were irradiated directly in the cavity of a Varian E-112 spectrometer with light from a Hanovia 1-kW high-pressure Hg–Xe lamp through Pyrex filters (3 mm). In each case, the solutions were prepared in Pyrex tubes by mixing equimolar amounts of HMB and HgT_2 in the appropriate solvent. The solutions were degassed by successive freeze–pump–thaw cycles and sealed in vacuo.

Charge-Transfer Photochemistry of the [HMB,HgT_2] Complex. Solution of HMB and HgT_2 in the appropriate solvent were degassed by successive freeze–pump–thaw cycles and sealed in vacuo in Pyrex vessels. They were irradiated either through interference filters (Melles Griot Co. F1U 023 and F1U 025) or more often through Pyrex filters with light from either a 1-kW Hg–Xe or 500-W xenon lamp. The pale yellow solution showed a sharp singlet in the ^1H NMR spectrum at δ 2.29 prior to photolysis. Irradiation caused this solution to turn deep blue ($HMB^{+\cdot}$) in 10–15 min with a small amount of grey solid apparent in trifluoroacetic acid. After photolysis, the singlet resonance at δ 2.29 was diminished and new singlet at δ 5.74 (2 H) and a pair of singlets [δ 2.36, 2.29 (15 H)] were observed, which corresponded to the spectrum of pentamethylbenzyl trifluoroacetate prepared independently by thallium(III) oxidation.[22a] Workup by an aqueous perchloric acid quench afforded a solution which was

(43) Maciel, G. E.; Borzo, M. *J. Magn. Reson.* **1973**, *10*, 388.

(44) We thank J. S. Frye (Colorado State University) for these studies.

quantitatively analyzed by GC–MS.

The mercurous trifluoroacetate $Hg_2(O_2CCF_3)_2$ which crystallized directly from dichloromethane in 90% yield was analyzed directly. Anal. Calcd for $HgO_2C_2F_3$: C, 7.66; F, 18.17. Found:[45] C, 7.91; F, 18.41. Mp 281–285 °C.

Quantum yield was determined by ferrioxalate actinometry[46] using light from a 500-W Eimac Xe lamp through interference filters (vide supra). The constant light intensity of this system was established by serially irradiating identical tubes for varying lengths of time. Typically the $Fe(Phen)_3^{3+}$ absorbance at λ 516 nm increased as follows with time (s): 0.48 (10), 0.83 (20), 1.23 (30), 1.72 (40), 1.83 (45). This shows a linear relationship of 0.15 einstein s^{-1} with a correlation coefficient of 0.9978.

Deuterium labeling studies were carried out with HMB-d_{18} and protio trifluoroacetic acid. Analysis of the products by GC–MS (Hewlett-Packard 5890-5790 B) showed the following cracking pattern for recovered HMB-d_{18}, m/z (relative intensity): 181 (6), 180 (50), 179 (10), 178 (4), 163 (11), 162 (100), 161 (18), 160 (1), 146 (3). These data compare with those of starting HMB-d_{18} of m/z (relative intensity) 181 (6), 180 (49), 179 (7), 178 (3), 163 (12), 162 (100), 161 (12), and 146 (2) and of the all protio-HMB of m/z (relative intensity) 163 (5), 162 (40), 161 (5), 148 (11), 147 (100), and 145 (2). The pentamethylbenzyl trifluoroacetate from the CT photochemistry of HMB-d_{18} showed the following mass spectrum, m/z (relative intensity): 292 (9), 291 (58), 290 (7), 179 (11), 178 (80), 177 (26), 176 (100), 175 (35). This compares with that derived from the all protio analogue, m/z (relative intensity): 275 (9), 274 (49), 162 (12), 161 (94), 160 (100), 148 (2), 147 (6), 146 (4), 145 (24). Thus the HMB-d_{18} recovered from the photolysis showed no evidence of proton exchange. However a comparison of the mass spectrum of the benzylic ester shows fragment ions with m/z 176 (100) and 178 (80) which are considered to be equivalent to 160 (100) and 161 (94) in the all protio analogue. Additional ions with m/z 175 (35) and 177 (26) can be accounted for if one of the 17 deuterium atoms has been replaced with a proton, i.e., $C_{14}D_{16}HF_3O_2$.

(45) Analysis performed by Galbraith Laboratories, Knoxville, TN.
(46) Calvert, J. G.; Pitts, J. N., Jr. *Photochemistry*; Wiley: New York, 1966.

Acknowledgment. We thank Halocarbon Products, Inc., for a generous supply of trifluoroacetic acid, Dr. J. C. Huffman for the X-ray structure in Figure 2, and the National Science Foundation and Robert A. Welch Foundation for financial support.

Registry No. HMB, 87-85-4; HgT_2, 13257-51-7; [HMB,HgT_2], 77001-38-8; Hg, 7439-97-6; ^{199}Hg, 14191-87-8; $HMB^{\bullet+}$, 34473-51-3; mercurous trifluoroacetate, 2923-15-1; pentamethylbenzyl trifluoroacetate, 35843-80-2.

Supplementary Material Available: Tables of the final atomic coordinates, bond lengths, bond angles, and anisotropic thermal parameters for the mercury(II) trifluoroacetate and hexamethylbenzene EDA complex (6 pages). Ordering information is given on any current masthead page.

Oxidation Studies on β-Lactam Antibiotics. The 6-(Diacylamino)penicillins

Ronald G. Micetich,*† Rajeshwar Singh,*† and Chia C. Shaw‡

Faculty of Pharmacy and Pharmaceutical Sciences, University of Alberta, Edmonton, Alberta, Canada T6G 2N8, and Ayerst Laboratories, Montreal, Quebec, Canada

Received August 6, 1985

The oxidation of the 6-(diacylamino)penicillins is a convenient, high yield route to the pencillin 1α-sulfoxides. The yield of the 1α-sulfoxide is dependent on the solvent, the temperature, the C-3 ester function, and the substituent at the C-2 position. The 6-(diacylamino)penicillin 1α-sulfoxides are readily converted to the penicillin 1α-sulfoxides on treatment with zinc and ammonium acetate.

The Morin rearrangements[1] of penicillin sulfoxides, **1**, to the desacetoxycephalosporins, **3**, has been shown to proceed via the azetidinone sulfenic acids, **2**.[2] This sigmatropic reaction is completely stereospecific, a proton from the C-2 methyl group cis to the sulfoxide S–O bond being abstracted to form the sulfenic acid, **2**. (See Scheme I.)

While unimportant in the case of penicillins (in which the *gem*-dimethyl groups are equivalent), this factor becomes significant in the case of the 2-(substituted-methyl)penicillins and the 2β-isomers, **4** (Scheme II), which are readily available.[3]

The 2β-(substituted-methyl)penicillin 1β-sulfoxides, **5**, are the major products formed by oxidation of compounds **4** (in which the C-6 substituent is an amide group) by the usual oxidants. This preferential formation of the 1β-sulfoxides, **5**, is explained by steric approach control, in which the amide proton bonds to the oxidant and, hence, directs the oxidation from the hindered β-face.[4] The thermolysis of these 2β-(substituted-methyl)penam 1β-sulfoxides, **5**, generates the vinylic azetidinone sulfenic acids, **6**.[5]

Table I. Percent α-Isomer[a,b] as a Function of Temperature[c]

substrate	reaction temp (°C)		
	−20 to −15	0	25
11a	44	58	76
11d	75	100	100

[a] Figures represent the average of three separate experiments. [b] Percent α-isomer is given on the basis of NMR; rest β-isomer formed. [c] Conditions: MCPBA/CH_2Cl_2/30 min.

(1) Morin, R. B.; Jackson, B. G.; Mueller, R. A.; Lavagnion, E. R.; Scanlon, W. B.; Andrews, S. L. *J. Am. Chem. Soc.* **1963**, *85*, 1896; **1969**, *91*, 1401.
(2) Cooper, R. D. G.; Spry, D. O. "Cephalosporin and Penicillin: Chemistry and Biology"; Flynn, E. H., Ed.; Academic Press: New York, 1972; 183–254.
(3) Kamiya, T.; Teraji, T.; Saito, Y.; Hashimoto, M.; Nakaguchi, O.; Oku, T. *Tetrahedron Lett.* **1973**, 3001.
(4) Cooper, R. D. G.; De marco, P. V.; Cheng, J. C.; Jones, N. D. *J. Am. Chem. Soc.* **1969**, *91*, 1408.
(5) Micetich, R. G., unpublished work.

† University of Alberta.
‡ Ayerst Laboratories.

0022-3263/86/1951-1811$01.50/0